Performance Analysis of Space-time Codes in Realistic Propagation Environments: A Moment Generating Function-Based Approach

Tharaka A. Lamahewa, Marvin K. Simon, Rodney A. Kennedy and Thushara D. Abhayapala

Abstract

In this paper, we derive analytical expressions for the exact pairwise error probability (PEP) of a space-time coded system operating over spatially correlated fast (constant over the duration of a symbol) and slow (constant over the length of a code word) fading channels using a moment-generating function-based approach. We discuss two analytical techniques that can be used to evaluate the exact-PEPs (and therefore approximate the average bit error probability (BEP)) in closed form. These analytical expressions are more realistic than previously published PEP expressions as they fully account for antenna spacing, antenna geometries (Uniform Linear Array, Uniform Grid Array, Uniform Circular Array, etc.) and scattering models (Uniform, Gaussian, Laplacian, Von-mises, etc). Inclusion of spatial information in these expressions provides valuable insights into the physical factors determining the performance of a space-time code. Using these new PEP expressions, we investigate the effect of antenna spacing, antenna geometries and azimuth power

This work was supported by the Australian Research Council Discovery Grant DP0343804.

T.A. Lamahewa, R.A. Kennedy and T.D. Abhayapala are with the Department of Telecommunications Engineering, Research School of Information Sciences and Engineering, the Australian National University, Canberra ACT 0200, Australia, email: {tharaka.lamahewa, rodney.kennedy, thushara.abhayapala}@anu.edu.au. M.K. Simon is with the Jet Propulsion Laboratory, California Institute of Technology, Pasadena, CA 91109, USA. email: marvin.k.simon@jpl.nasa.gov. R.A. Kennedy and T.D. Abhayapala are also with National ICT Australia, Locked Bag 8001, Canberra, ACT 2601, AUSTRALIA. National ICT Australia is funded through the Australian Government's *Backing Australia's Ability* initiative, in part through the Australian Research Council.

Part of this paper has been submitted to 3rd Workshop on the Internet, Telecommunications, and Signal Processing, WITSP-2004, Adelaide, Australia.

distribution parameters (angle of arrival/departure and angular spread) on the performance of a four-state QPSK space-time trellis code proposed by Tarokh et al. for two transmit antennas.

Index Terms

Gaussian Q-function, modal correlation, moment-generating function, MIMO system, non-isotropic scattering, space-time coding.

I. INTRODUCTION

Space-time coding combines channel coding with multiple transmit and multiple receive antennas to achieve bandwidth and power efficient high data rate transmission over fading channels. The performance criteria for space-time codes have been derived in [1] based on the Chernoff bound applied to the pairwise error probability (PEP). In [2, 3], the average bit error probability (BEP) of space-time trellis codes was evaluated using the traditional Chernoff bounding technique on the PEP. In general, the Chernoff bound is quite loose for low signal-to-noise ratios. In [4], the exact-PEP of space-time codes operating over independent and identically distributed (i.i.d.) fast fading channels was derived using the method of residues. A simple method for exactly evaluating the PEP (and approximate BEP) based on the moment generating function associated with a quadratic form of a complex Gaussian random variable [5] is given in [6] for both i.i.d. slow and fast fading channels.

When designing space-time codes, the main assumption being made is that the channel gains between the transmitter and the receiver antennas undergo independent fading. However, independent fading models an unrealistic propagation environment. The spatial fading correlation effects on the exact-PEP of space-time codes were investigated in [7]. There, the exact-PEP results derived in [4] were further extended to spatially correlated slow fading channels with the use of residue methods. In [7], the correlation is calculated in terms of the correlation between channel gains, but there is no direct realizable physical interpretation to the spatial correlation. Therefore, existing PEP expressions derived in the literature do not provide insights into the physical factors determining the performance of a space-time code over correlated fading channels. In particular, the effect of antenna spacing, spatial geometry of the antenna arrays and the non-isotropic scattering environments on the performance of space-time codes are of interest.

In this paper, using the MGF-based approach presented in [6], we derive analytical expressions for the exact-PEP (and approximate BEP) of a space-time coded system over spatially

correlated fast and slow fading channels. These expressions are more realistic than previously published [4, 6, 7] exact-PEP expressions, as they fully account for antenna placement along with non-isotropic scattering environments. Using these analytical expressions one can evaluate the performance of a space-time code applied to a MIMO system in any general spatial scenario (*antenna geometries*: Uniform Linear Array (ULA), Uniform Grid Array (UGA), Uniform Circular Array (UCA), etc. *scattering models*: Uniform, Gaussian, Laplacian, Von-mises, etc.) without the need for extensive simulations. We discuss two analytical techniques that can be used to evaluate the exact-PEPs (and therefore approximate the average BEP) in closed form, namely, (a)-*Direct partial fraction expansion* (b)-*Partial fraction expansion via eigenvalue decomposition*. We demonstrate the strength of these new analytical PEP expressions by evaluating the performance of a four-state QPSK space-time trellis code with two transmit antennas proposed by Tarokh et al. [1] for different spatial scenarios.

II. System Model

Notations: Throughout the paper, the following notations will be used: $[\cdot]^T$, $[\cdot]^*$ and $[\cdot]^\dagger$ denote the transpose, complex conjugate and conjugate transpose operations, respectively. The symbols $\delta(\cdot)$ and $\otimes$ denote the Dirac delta function and Matrix Kronecker product, respectively. The notation $\|\cdot\|^2$ denotes the squared norm of a matrix: $\|\boldsymbol{X}_{P\times Q}\|^2 = \sum_{i=1}^{P}\sum_{j=1}^{Q}|a_{ij}|^2$, $E\{\cdot\}$ denotes the mathematical expectation, $\mathrm{vec}(\boldsymbol{A})$ denotes the vectorization operator which stacks the columns of $\boldsymbol{A}$, and $\lceil . \rceil$ denotes the ceiling operator. The matrix $\boldsymbol{I}_n$ is the $n \times n$ identity matrix.

Consider a MIMO system consisting of n_T transmit antennas and n_R receive antennas. Let $\boldsymbol{x}_n = [x_1^{(n)}, x_2^{(n)}, \cdots x_{n_T}^{(n)}]^T$ denote the space-time coded signal vector transmitted from n_T transmit antennas in the n-th symbol interval. Let $\boldsymbol{X} = [\boldsymbol{x}_1, \boldsymbol{x}_2, \cdots, \boldsymbol{x}_L]$ denote the space-time code representing the entire transmitted signal, where L is the code length. The received signal at the q-th receive antenna in the n-th symbol interval is given by

$$r_q^{(n)} = \sqrt{E_s}\sum_{p=1}^{n_T} h_{q,p}^{(n)} x_p^{(n)} + \eta_q^{(n)},$$

$$q = 1, 2, \cdots, n_R, \;\; n = 1, 2, \cdots, L, \tag{1}$$

where E_s is the transmitted power per symbol at each transmit antenna and $\eta_q^{(n)}$ is the additive noise on the q-th receive antenna at symbol interval n. The additive noise is assumed to be

white and complex Gaussian distributed with mean zero and variance $N_0/2$ per dimension. Here the coefficient $h_{q,p}^{(n)}$ represents the random complex channel gain between the p-th transmit antenna and the q-th receive antenna. Let $\boldsymbol{H}_n = [h_{q,p}]$ denote the $n_R \times n_T$ channel gain matrix associated with the n-th symbol interval.

By taking into account the physical aspects of scattering, the channel matrix $\boldsymbol{H}_n$ can be decomposed into deterministic and random parts as [8–10]

$$\boldsymbol{H}_n = \boldsymbol{J}_R \boldsymbol{S}_n \boldsymbol{J}_T^{\dagger}, \tag{2}$$

where the matrices $\boldsymbol{J}_R$ and $\boldsymbol{J}_T$ are deterministic and $\boldsymbol{S}_n$ is random. According to the channel model proposed in [8], $\boldsymbol{S}_n$ is the i.i.d. channel matrix associated with the n-th symbol interval, which has zero-mean and unit variance complex Gaussian entries, while $\boldsymbol{J}_R$ and $\boldsymbol{J}_T$ are the receive and transmit antenna correlation matrices, respectively. For the channel models proposed in [9] and [10], $\boldsymbol{S}_n$ represents the random scattering environment associated with the n-th symbol interval and $\boldsymbol{J}_R$ and $\boldsymbol{J}_T$ represent the antenna configurations at the receive and transmit antenna arrays, respectively.

In this work, we are mainly interested in investigating the impact of antenna separation, antenna geometry and the general scattering environment on the performance of a space-time coded system. The channel model given in [8] is restricted to a uniform linear array antenna configuration and a countable number of scatterers around the transmit and receive antenna arrays. However, the channel models given in [9, 10], are capable of capturing different antenna geometries as well as various non-isotropic power distributions around the transmit and receive antenna arrays. Here we only consider planar antenna arrays and a 2-dimensional scattering environment. Therefore we use the 2-dimensional spatial channel model[1] proposed in [9] for our PEP investigations.

A. Spatial Channel Model

Using a recently developed spatial channel model [9], we are able to incorporate the antenna spacing, antenna geometries and scattering distribution parameters such as the mean angle-of-arrival (AOA), mean angle-of-departure (AOD) and the angular spread into the exact-PEP calculations of space-time coded systems. In this model, the MIMO channel is separated into three physical regions of interest: the scatterer-free region around the transmit antenna array,

[1] The 2-dimensional case is a special case of the 3-dimensional case where all the signals arrive from on a horizontal plane only. Similar results can be obtained using the 3-dimensional channel model proposed in [10].

the scatterer-free region around the receive antenna array and the complex random scattering media which is the complement of the union of two antenna array regions. This separation of regions leads to the decomposition in (2) which will play a key role in this paper.

Here $\boldsymbol{J}_T$ is the $n_T \times (2m_T + 1)$ transmit antenna array configuration matrix and $\boldsymbol{J}_R$ is the $n_R \times (2m_R+1)$ receive antenna array configuration matrix, where $(2m_T+1)$ and $(2m_R+1)$ are the number of effective communication modes available in the transmit and receive regions, respectively. Note that, m_T and m_R are determined by the size of the antenna aperture [11], but not from the number of antennas encompassed in an antenna array. The precise definitions of $\boldsymbol{J}_R$ and $\boldsymbol{J}_T$ are given in Appendix I.

$\boldsymbol{S}_n$ is the $(2m_R + 1) \times (2m_T + 1)$ random scattering matrix with (ℓ, m)-th element given by

$$\{\boldsymbol{S}_n\}_{\ell,m} = \int_0^{\pi} \int_0^{\pi} g_n(\phi, \varphi) e^{-i(\ell - m_R - 1)\varphi} e^{i(m - m_T - 1)\phi} d\varphi d\phi,$$
$$\ell = 1, \cdots, 2m_R + 1, \quad m = 1, \cdots, 2m_T + 1 \tag{3}$$

Note that $\{\boldsymbol{S}_n\}_{\ell,m}$ represents the complex gain of the scattering channel between the m-th mode[2] of the transmit region and the ℓ-th mode of the receive region, where $g_n(\phi, \varphi)$ is the scattering gain function, which is the effective random complex gain for signals leaving the transmit aperture with angle of departure ϕ and arriving at the receive aperture with angle of arrival φ over the n-th symbol interval.

III. Exact PEP on Correlated MIMO Channels

Assume that perfect channel state information (CSI) is available at the receiver and a maximum likelihood (ML) decoder is employed at the receiver. Assume that the codeword $\boldsymbol{X}$ was transmitted, but the ML-decoder chooses another codeword $\hat{\boldsymbol{X}}$. Then the PEP, conditioned on the channel, is given by [1]

$$\mathrm{P}(\boldsymbol{X} \to \hat{\boldsymbol{X}} | \boldsymbol{H}_n) = \mathrm{Q}\left(\sqrt{\frac{E_s}{2N_0} d^2}\right), \tag{4}$$

[2]The set of modes form a basis of functions for representing a multipath wave field.

where $\mathrm{Q}(y) = \int_{-\infty}^{y} e^{-x^2/2}\mathrm{dx}$, is the Gaussian Q-function and d is the Euclidian distance. In the case of a time-varying fading channel,

$$\begin{aligned} d^2 &= \sum_{n=1}^{L} \|\boldsymbol{H}_n(\boldsymbol{x}_n - \hat{\boldsymbol{x}}_n)\|^2, \\ &= \sum_{n=1}^{L} \boldsymbol{h}_n[\boldsymbol{I}_{n_R} \otimes \boldsymbol{x}_{\Delta}^n]\boldsymbol{h}_n^{\dagger}, \end{aligned} \tag{5}$$

where $\boldsymbol{x}_{\Delta}^n = (\boldsymbol{x}_n - \hat{\boldsymbol{x}}_n)(\boldsymbol{x}_n - \hat{\boldsymbol{x}}_n)^{\dagger}$ and $\boldsymbol{h}_n = \left(\mathrm{vec}\left(\boldsymbol{H}_n^T\right)\right)^T$ is a row vector. For a slow fading channel (quasi-static fading), we would have $\boldsymbol{H}_n = \boldsymbol{H}$ for $n = 1, 2, \cdots, L$, then d^2 simplifies to

$$\begin{aligned} d^2 &= \|\boldsymbol{H}(\boldsymbol{X} - \hat{\boldsymbol{X}})\|^2, \\ &= \boldsymbol{h}[\boldsymbol{I}_{n_R} \otimes \boldsymbol{X}_{\Delta}]\boldsymbol{h}^{\dagger}, \end{aligned} \tag{6}$$

where $\boldsymbol{X}_{\Delta} = (\boldsymbol{X} - \hat{\boldsymbol{X}})(\boldsymbol{X} - \hat{\boldsymbol{X}})^{\dagger}$ and $\boldsymbol{h} = \left(\mathrm{vec}\left(\boldsymbol{H}^T\right)\right)^T$ is a row vector. Note also that $\boldsymbol{X}_{\Delta} = \sum_{n=1}^{L} \boldsymbol{x}_{\Delta}^n$.

To compute the average PEP, we average (4) over the joint probability distribution of the channel gains. By using Craig's formula for the Gaussian Q-function [12]

$$\mathrm{Q}(x) = \frac{1}{\pi}\int_0^{\pi/2} \exp\left(-\frac{x^2}{2\sin^2\theta}\right)\mathrm{d}\theta$$

and the MGF-based technique presented in [6], we can write the average PEP as

$$\begin{aligned} \mathrm{P}(\boldsymbol{X} \to \hat{\boldsymbol{X}}) &= \frac{1}{\pi}\int_0^{\pi/2}\int_0^{\infty} \exp\left(-\frac{\Gamma}{2\sin^2\theta}\right) p_{\Gamma}(\Gamma)d\Gamma\mathrm{d}\theta, \\ &= \frac{1}{\pi}\int_0^{\pi/2} \mathcal{M}_{\Gamma}\left(-\frac{1}{2\sin^2\theta}\right)\mathrm{d}\theta, \end{aligned} \tag{7}$$

where $\mathcal{M}_{\Gamma}(s) \triangleq \int_0^{\infty} e^{s\Gamma} p_{\Gamma}(\Gamma)d\Gamma$ is the MGF of

$$\Gamma = \frac{E_s}{2N_0}d^2 \tag{8}$$

and $p_{\Gamma}(\Gamma)$ is the probability density function (pdf) of Γ.

A. Fast Fading Channel Model

In this section, we derive the exact-PEP of a space-time coded system applied to a spatially correlated fast fading MIMO channel.

Substituting (2) for $\boldsymbol{H}_n$ in $\boldsymbol{h}_n = (\mathrm{vec}\,(\boldsymbol{H}_n^T))^T$ and using the Kronecker product identity [13, page 180] $\mathrm{vec}(\boldsymbol{AXB}) = (\boldsymbol{B}^T \otimes \boldsymbol{A})\,\mathrm{vec}\,(\boldsymbol{X})$, we re-write (5) as

$$d^2 = \sum_{n=1}^{L} \boldsymbol{s}_n (\boldsymbol{J}_R^T \otimes \boldsymbol{J}_T^\dagger)(\boldsymbol{I}_{n_R} \otimes \boldsymbol{x}_\Delta^n)(\boldsymbol{J}_R^* \otimes \boldsymbol{J}_T)\boldsymbol{s}_n^\dagger, \tag{9a}$$

$$= \sum_{n=1}^{L} \boldsymbol{s}_n \left[(\boldsymbol{J}_R^\dagger \boldsymbol{J}_R)^T \otimes (\boldsymbol{J}_T^\dagger \boldsymbol{x}_\Delta^n \boldsymbol{J}_T) \right] \boldsymbol{s}_n^\dagger, \tag{9b}$$

$$= \sum_{n=1}^{L} \boldsymbol{s}_n \boldsymbol{G}_n \boldsymbol{s}_n^\dagger, \tag{9c}$$

where $\boldsymbol{s}_n = (\mathrm{vec}(\boldsymbol{S}_n^T))^T$ is a row vector and

$$\boldsymbol{G}_n = (\boldsymbol{J}_R^\dagger \boldsymbol{J}_R)^T \otimes (\boldsymbol{J}_T^\dagger \boldsymbol{x}_\Delta^n \boldsymbol{J}_T). \tag{10}$$

Note that, (9b) follows from (9a) via the identity [13, page 180] $(\boldsymbol{A} \otimes \boldsymbol{C})(\boldsymbol{B} \otimes \boldsymbol{D}) = \boldsymbol{AB} \otimes \boldsymbol{CD}$, provided that the matrix products $\boldsymbol{AB}$ and $\boldsymbol{CD}$ exist. Substituting (9c) in (8), we get

$$\Gamma = \frac{E_s}{2N_0} \sum_{n=1}^{L} \boldsymbol{s}_n \boldsymbol{G}_n \boldsymbol{s}_n^\dagger. \tag{11}$$

Since $\boldsymbol{s}_n$ is a random row vector and $\boldsymbol{G}_n$ is fixed as $\boldsymbol{J}_T, \boldsymbol{J}_R$ and $\boldsymbol{x}_\Delta^n$ are deterministic matrices, then Γ is a random variable too. In fact, $\boldsymbol{s}_n \boldsymbol{G}_n \boldsymbol{s}_n^\dagger$ is a quadratic form of a random variable. Now we illustrate how one would find the MGF of Γ in (11) for a fast fading channel.

Using the standard definition of the MGF, we can write

$$\mathcal{M}_\Gamma(s) = E\left\{ \exp\left(s \frac{E_s}{2N_0} \sum_{n=1}^{L} \boldsymbol{s}_n \boldsymbol{G}_n \boldsymbol{s}_n^\dagger \right) \right\},$$

$$= E\left\{ \prod_{n=1}^{L} \exp\left(s \frac{E_s}{2N_0} \boldsymbol{s}_n \boldsymbol{G}_n \boldsymbol{s}_n^\dagger \right) \right\}. \tag{12}$$

Assume that $\boldsymbol{s}_n$ is a proper-complex Gaussian random row-vector (properties associated with proper-complex Gaussian vectors are given in [14]) with mean zero and covariance $\boldsymbol{R}_n$ defined as $E\left\{\boldsymbol{s}_n^\dagger \boldsymbol{s}_n\right\}$. Let $p(\boldsymbol{s}_1, \boldsymbol{s}_2, \cdots, \boldsymbol{s}_L)$ denote the joint pdf of $\boldsymbol{s} = (\boldsymbol{s}_1, \boldsymbol{s}_2, \cdots, \boldsymbol{s}_L)$. Then, we get

$$\mathcal{M}_\Gamma(s) = \int_{\boldsymbol{V}} \prod_{n=1}^{L} \exp\left(s \frac{E_s}{2N_0} \boldsymbol{s}_n \boldsymbol{G}_n \boldsymbol{s}_n^\dagger \right) p(\boldsymbol{s}_1, \boldsymbol{s}_2, \cdots, \boldsymbol{s}_L) \mathrm{d}\boldsymbol{V}, \tag{13}$$

where we have introduced the following two shorthand notations

$$\int_{\boldsymbol{V}} \mathrm{d}\boldsymbol{V} \triangleq \int_{\boldsymbol{V}_1}\int_{\boldsymbol{V}_2}\cdots\int_{\boldsymbol{V}_L} \mathrm{d}\boldsymbol{V}_1\mathrm{d}\boldsymbol{V}_2\cdots\mathrm{d}\boldsymbol{V}_{\mathrm{L}},$$

$$\mathrm{d}\boldsymbol{V}_{\mathrm{n}} = \prod_{\ell=1}^{K} \mathrm{d}s_{n\ell}^{R}\mathrm{d}s_{n\ell}^{I},$$

where $s_{n\ell}^{R}$ and $s_{n\ell}^{I}$ are the real and imaginary parts of the ℓ-th element of the vector $\boldsymbol{s}_n$, respectively and $K = (2m_R+1)(2m_T+1)$ is the length of $\boldsymbol{s}_n$.

In this work, we are mainly interested in investigating the spatial correlation effects of the scattering environment on the performance of space-time codes. Therefore, we can assume that the temporal correlation of the scattering environment is zero, i.e.

$$E\left\{\boldsymbol{s}_n^{\dagger}\boldsymbol{s}_m\right\} = \begin{cases} \boldsymbol{R}_n, & n = m; \\ \boldsymbol{0}, & n \neq m. \end{cases}$$

$$\text{for } n, m = 1, 2, \cdots, L. \tag{14}$$

Assuming now that the scattering environment is temporally uncorrelated, and as a result $p(\boldsymbol{s}_1, \boldsymbol{s}_2, \cdots, \boldsymbol{s}_L) = \prod_{n=1}^{L} p(\boldsymbol{s}_n)$, we can write the MGF of Γ as

$$\begin{aligned}\mathcal{M}_{\Gamma}(s) &= \prod_{n=1}^{L}\int_{\boldsymbol{V}_n} \exp\left(s\frac{E_s}{2N_0}\boldsymbol{s}_n\boldsymbol{G}_n\boldsymbol{s}_n^{\dagger}\right) p(\boldsymbol{s}_n)\mathrm{d}\boldsymbol{V}_n, \\ &= \prod_{n=1}^{L}\mathcal{M}_{\Gamma_n}(s), \end{aligned} \tag{15}$$

where

$$\Gamma_n = \frac{E_s}{2N_0}\boldsymbol{s}_n\boldsymbol{G}_n\boldsymbol{s}_n^{\dagger}.$$

Here the $2LK$-th order integral in (13) reduces to a product of L $2K$-th order integrals, each corresponding to the MGF of one of the Γ_n, where Γ_n is a quadratic form of a random variable. The MGF associated with a quadratic random variable is readily found in the literature [5]. Here we present the basic result given in Turin [5] on MGF of a quadratic random variable as follows.

Let $\boldsymbol{Q}$ be a Hermitian matrix and $\boldsymbol{v}$ be a proper complex normal zero-mean Gaussian row vector with covariance matrix $\boldsymbol{L} = E\left\{\boldsymbol{v}^{\dagger}\boldsymbol{v}\right\}$. Then the MGF of the (real) quadratic form $f = \boldsymbol{v}\boldsymbol{Q}\boldsymbol{v}^{\dagger}$ is given by

$$\mathcal{M}_f(s) = \left[\det\left(\boldsymbol{I} - s\boldsymbol{L}\boldsymbol{Q}\right)\right]^{-1}. \tag{16}$$

In our case, $\boldsymbol{G}_n$ is a Hermitian matrix (the proof is given in Appendix-II). Therefore, using (16) we write the MGF of Γ_n as

$$\mathcal{M}_{\Gamma_n}(s) = \left[\det\left(\boldsymbol{I} - \frac{s\bar{\gamma}}{2}\boldsymbol{R}_n\boldsymbol{G}_n\right)\right]^{-1}, \tag{17}$$

where $\bar{\gamma} = \frac{E_s}{N_0}$ is the average symbol energy-to-noise ratio (SNR), $\boldsymbol{R}_n$ is the covariance matrix of $\boldsymbol{s}_n$ as defined in (14) and $\boldsymbol{G}_n$ is given in (10). Substituting (17) in (15) and then the result in (7) yields the exact-PEP

$$\mathrm{P}(\boldsymbol{X} \to \hat{\boldsymbol{X}}) = \frac{1}{\pi}\int_0^{\pi/2}\prod_{n=1}^{L}\left[\det\left(\boldsymbol{I} + \frac{\bar{\gamma}}{4\sin^2\theta}\boldsymbol{R}_n\boldsymbol{G}_n\right)\right]^{-1}\mathrm{d}\theta. \tag{18}$$

Remark 1: Eq. (18) is the exact-PEP[3] of a space-time coded system applied to a spatially-correlated fast fading channel following the channel decomposition in (2).

Remark 2: When $\boldsymbol{R}_n = \boldsymbol{I}$ (i.e., correlation between different communication modes is zero), Eq. (18) above captures the effects due to antenna spacing and antenna geometry on the performance of a space-time code over a fast fading channel.

Remark 3: When the fading channels are independent (i.e., $\boldsymbol{R}_n = \boldsymbol{I}$ and $\boldsymbol{G}_n = \boldsymbol{I}_{n_R} \otimes \boldsymbol{x}_\Delta^n$), (18) simplifies to,

$$\mathrm{P}(\boldsymbol{X} \to \hat{\boldsymbol{X}}) = \frac{1}{\pi}\int_0^{\pi/2}\prod_{n=1}^{L}\left[\det\left(\boldsymbol{I}_{n_T} + \frac{\bar{\gamma}}{4\sin^2\theta}\boldsymbol{x}_\Delta^n\right)\right]^{-n_R}\mathrm{d}\theta,$$

which is the same as [6, Eq. (9)].

In the next section, we derive the exact-PEP of a space-time coded system for a slow quasi-static fading channel. Note that, we are not able to use the fast fading result (18) to obtain the exact-PEP for a slow fading channel. This is because we derived (18) under the assumption of a temporally uncorrelated scattering environment. In contrast, for a slow fading channel, the scattering environment is fully temporally correlated.

B. Slow Fading Channel Model

For a slow fading channel, $\boldsymbol{H}_n = \boldsymbol{H}$ independent of n in which case (8) becomes

$$\Gamma = \frac{E_s}{2N_0}\boldsymbol{s}\boldsymbol{G}\boldsymbol{s}^\dagger, \tag{19}$$

[3]Eq. (18) can be evaluated in closed form using one of the analytical techniques discussed in Section IV.

where $\boldsymbol{s} = (\mathrm{vec}(\boldsymbol{S}^T))^T$ is a row vector with proper complex normal Gaussian distributed entries and

$$\boldsymbol{G} = (\boldsymbol{J}_R^\dagger \boldsymbol{J}_R)^T \otimes (\boldsymbol{J}_T^\dagger \boldsymbol{X}_\Delta \boldsymbol{J}_T). \tag{20}$$

As before, Γ is a random variable that has a quadratic form. Since $\boldsymbol{G}$ in (20) is Hermitian (as shown in Appendix II), using (16), we can write the MGF of Γ as

$$\mathcal{M}_\Gamma(s) = \left[\det\left(\boldsymbol{I} - \frac{s\bar{\gamma}}{2}\boldsymbol{R}\boldsymbol{G}\right)\right]^{-1}, \tag{21}$$

where $\boldsymbol{R}$ is the covariance matrix of the scattering environment which is defined as $\boldsymbol{R} = E\left\{\boldsymbol{s}^\dagger \boldsymbol{s}\right\}$. Substitution of (21) into (7) yields

$$\mathrm{P}(\boldsymbol{X} \to \hat{\boldsymbol{X}}) = \frac{1}{\pi}\int_0^{\pi/2} \left[\det\left(\boldsymbol{I} + \frac{\bar{\gamma}}{4\sin^2\theta}\boldsymbol{R}\boldsymbol{G}\right)\right]^{-1} \mathrm{d}\theta. \tag{22}$$

Remark 4: Eq (22) is the exact-PEP of a space-time coded system applied to a spatially correlated slow fading MIMO channel following the channel decomposition in (2).

Remark 5: When the fading channels are independent (i.e., $\boldsymbol{R} = \boldsymbol{I}$ and $\boldsymbol{G} = \boldsymbol{I}_{n_R} \otimes \boldsymbol{X}_\Delta$), (22) simplifies to,

$$\mathrm{P}(\boldsymbol{X} \to \hat{\boldsymbol{X}}) = \frac{1}{\pi}\int_0^{\pi/2} \prod_{n=1}^{L} \left[\det\left(\boldsymbol{I}_{n_T} + \frac{\bar{\gamma}}{4\sin^2\theta}\boldsymbol{X}_\Delta\right)\right]^{-n_R} \mathrm{d}\theta,$$

which is the same as [6, Eq. (13)].

C. Kronecker Product Model as a Special Case

In some circumstances, the covariance matrix $\boldsymbol{R}_n$ of the scattering channel can be expressed as a Kronecker product between correlation matrices observed at the receiver and the transmitter antenna arrays [15, 16], i.e.,

$$\boldsymbol{R}_n = E\left\{\boldsymbol{s}_n^\dagger \boldsymbol{s}_n\right\} = \boldsymbol{F}_n^R \otimes \boldsymbol{F}_n^T, \tag{23}$$

where $\boldsymbol{F}_n^R$ and $\boldsymbol{F}_n^T$ are the transmit and receive correlation matrices associated with the n-th symbol interval. Substituting (23) in (18) and recalling the definition of $\boldsymbol{G}_n$ in (10), we can simplify the exact-PEP for the fast fading channel to

$$\mathrm{P}(\boldsymbol{X} \to \hat{\boldsymbol{X}}) = \frac{1}{\pi}\int_0^{\pi/2} \prod_{n=1}^{L} \left[\det\left(\boldsymbol{I} + \frac{\bar{\gamma}}{4\sin^2\theta}\boldsymbol{Z}_n\right)\right]^{-1} \mathrm{d}\theta. \tag{24}$$

where $\boldsymbol{Z}_n = (\boldsymbol{F}_n^R \boldsymbol{J}_R^T \boldsymbol{J}_R^*) \otimes (\boldsymbol{F}_n^T \boldsymbol{J}_T^\dagger \boldsymbol{x}_\Delta^n \boldsymbol{J}_T)$. Similarly, for the slow fading channel, we can factor $\boldsymbol{R}$ as

$$\boldsymbol{R} = E\left\{\boldsymbol{s}^\dagger \boldsymbol{s}\right\} = \boldsymbol{F}^R \otimes \boldsymbol{F}^T, \tag{25}$$

and then the exact-PEP can be expressed as

$$\mathrm{P}(\boldsymbol{X} \to \hat{\boldsymbol{X}}) = \frac{1}{\pi} \int_0^{\pi/2} \left[\det\left(\boldsymbol{I} + \frac{\bar{\gamma}}{4\sin^2\theta} \boldsymbol{Z}\right)\right]^{-1} \mathrm{d}\theta \tag{26}$$

where $\boldsymbol{Z} = (\boldsymbol{F}^R \boldsymbol{J}_R^T \boldsymbol{J}_R^*) \otimes (\boldsymbol{F}^T \boldsymbol{J}_T^\dagger \boldsymbol{X}_\Delta \boldsymbol{J}_T)$.

In section VII, we provide the necessary condition which a scattering channel must satisfy in order for the factorizations (23) and (25) above to hold. There we also define the transmit and receive correlation matrices associated with the channel model [9]. The pairwise error probability expressions (24) and (26) will be used later in our simulations to investigate the effects of correlation on the performance of space-time codes.

IV. Realistic Exact-PEP

The exact-PEP expressions we derived in Sections III-A and III-B for the fast fading and slow fading MIMO channels, respectively capture the antenna configurations (Linear Array, Circular Array, Grid, etc.) both at the transmitter and the receiver arrays via $\boldsymbol{J}_T$ and $\boldsymbol{J}_R$, respectively. These expressions also incorporate the spatial correlation effects at the transmitter and the receiver regions via $\boldsymbol{F}_n^T$, $\boldsymbol{F}_n^R$ for the fast fading case and via $\boldsymbol{F}^T$ and $\boldsymbol{F}^R$ for the slow fading case. Therefore, PEP expressions (24) and (26) are the ***realistic*** exact-PEPs of space-time coded systems for the fast fading and slow fading MIMO channels, respectively.

To calculate the exact-PEP, one needs to evaluate the integrals (24) and (26), either using numerical methods or analytical methods. In the following sections, we present two analytical techniques which can be employed to evaluate the integrals (24) and (26) in closed form, namely (a)-*Direct partial fraction expansion* (b)-*Partial fraction expansion via eigenvalue decomposition*. The technique-(b) was previously reported in [17]. We shall use (26), which is the integral involved with the slow fading channel model, to introduce these two techniques. Note that both methods can be directly applied to evaluate the integral involved with the fast fading channel; therefore we omit the details here for the sake of brevity.

A. Direct Partial Fraction Expansion

Matrix $\boldsymbol{Z}$ in (26) has size $M_R M_T \times M_R M_T$, where $M_R = 2m_R + 1$ and $M_T = 2m_T + 1$. Therefore, the integrand in (26) will take the form[4]

$$\left[\det\left(\boldsymbol{I} + \frac{\bar{\gamma}}{4\sin^2\theta}\boldsymbol{Z}\right)\right]^{-1} = \frac{(\sin^2\theta)^N}{\sum_{\ell=0}^{N} a_\ell (\sin^2\theta)^\ell}, \tag{27}$$

where $N = M_R M_T$ and a_ℓ, for $\ell = 1, 2, \cdots, N$, are constants. Note that the denominator of (27) is an N-th order polynomial in $\sin^2\theta$ (for the fast fading channel, it would be an LN-th order polynomial). To evaluate the integral (27) in closed form, we use the partial-fraction expansion technique given in [18, Appendix 5A] as follows.

First we begin by factoring the denominator of (27) into terms of the form $(\sin^2\theta + c_\ell)$, for $\ell = 1, 2, \cdots, N$. This involves finding the roots of an N-th order polynomial in $\sin^2\theta$ either numerically or analytically. Then (27) can be expressed in product form as

$$\frac{(\sin^2\theta)^N}{\sum_{\ell=0}^{N} a_\ell (\sin^2\theta)^\ell} = \prod_{\ell=1}^{\Lambda}\left(\frac{\sin^2\theta}{c_\ell + \sin^2\theta}\right)^{m_\ell} \tag{28}$$

where m_ℓ is the multiplicity of the root c_ℓ and $\sum_{\ell=1}^{\Lambda} m_\ell = N$. Applying the partial-fraction decomposition theorem to the product form (28), we get

$$\prod_{\ell=1}^{\Lambda}\left(\frac{\sin^2\theta}{c_\ell + \sin^2\theta}\right)^{m_\ell} = \sum_{\ell=1}^{\Lambda}\sum_{k=1}^{m_\ell} A_{k\ell}\left(\frac{\sin^2\theta}{c_\ell + \sin^2\theta}\right)^{k} \tag{29}$$

where the residual $A_{k\ell}$ is given by [18, Eq. 5A.72]

$$A_{k\ell} = \frac{\left\{\frac{d^{m_\ell - k}}{dx^{m_\ell - k}}\prod_{\substack{n=1\\ n\neq\ell}}^{\Lambda}\left(\frac{1}{1+c_n x}\right)^{m_n}\right\}\Big|_{x=-c_\ell^{-1}}}{(m_\ell - k)! c_\ell^{m_\ell - k}}. \tag{30}$$

Expansion (29) often allows integration to be performed on each term separately by inspection. In fact, each term in (29) can be separately integrated using a result found in [6], where

$$\begin{aligned} P(c_\ell, k) &= \frac{1}{\pi}\int_0^{\pi/2}\left(\frac{\sin^2\theta}{c_\ell + \sin^2\theta}\right)^k \mathrm{d}\theta, \\ &= \left[1 - \sqrt{\frac{c_\ell}{1+c_\ell}}\sum_{j=0}^{k-1}\binom{2j}{j}\left(\frac{1}{4(1+c_\ell)}\right)^j\right]. \end{aligned} \tag{31}$$

[4]One would need to evaluate the determinant of $\left(\boldsymbol{I} + \frac{\bar{\gamma}}{4\sin^2\theta}\boldsymbol{Z}\right)$ and then take the reciprocal of it to obtain the form (27).

Now using the partial-fraction form of the integrand in (29) together with (31), we obtain the exact-PEP in closed form as

$$\begin{aligned}\mathrm{P}(\boldsymbol{X} \to \hat{\boldsymbol{X}}) &= \frac{1}{\pi}\int_0^{\pi/2}\prod_{\ell=1}^{\Lambda}\left(\frac{\sin^2\theta}{c_\ell+\sin^2\theta}\right)^{m_\ell}\mathrm{d}\theta,\\ &= \frac{1}{2}\sum_{\ell=1}^{\Lambda}\sum_{k=1}^{m_\ell}A_{k\ell}P(c_\ell,k). \end{aligned} \tag{32}$$

For the special case of distinct roots, i.e., $m_1 = m_2 = \cdots = m_N = 1$, the exact-PEP is given by

$$\mathrm{P}(\boldsymbol{X} \to \hat{\boldsymbol{X}}) = \frac{1}{2}\sum_{\ell=1}^{N}\left(1-\sqrt{\frac{c_\ell}{1+c_\ell}}\right)\prod_{\substack{n=1\\ n\neq\ell}}^{N}\left(\frac{c_\ell}{c_\ell-c_n}\right).$$

B. Partial Fraction Expansion via Eigenvalue Decomposition

The main difficulty with the above technique is finding the roots of an N-th order polynomial. Here we provide a rather simple way to evaluate the exact-PEP in closed form using an eigenvalue decomposition technique. However, this technique also makes use of the partial fraction expansion technique given in [18, Appendix 5A].

Let $\bar{\boldsymbol{Z}} = \frac{\bar{\gamma}}{4}\boldsymbol{Z}$, where $\boldsymbol{Z}$ is the matrix defined in (27). Suppose matrix $\bar{\boldsymbol{Z}}$ has K non-zero eigenvalues, including multiplicity, $\lambda_1, \lambda_2, \cdots, \lambda_K$, and the decomposition $\bar{\boldsymbol{Z}} = \boldsymbol{A}\boldsymbol{D}\boldsymbol{A}^{-1}$, where $\boldsymbol{A}$ is the matrix of eigenvectors of $\bar{\boldsymbol{Z}}$ and $\boldsymbol{D}$ is a diagonal matrix with the eigenvalues of $\bar{\boldsymbol{Z}}$ on the diagonal. Then the integrand in (26) can be written as

$$\begin{aligned}\left[\det\left(\boldsymbol{I}+\frac{\bar{\gamma}}{4\sin^2\theta}\boldsymbol{Z}\right)\right]^{-1} &= \left[\det\left(\boldsymbol{I}+\frac{1}{\sin^2\theta}\boldsymbol{D}\right)\right]^{-1},\\ &= \prod_{\ell=1}^{K}\left(\frac{\sin^2\theta}{\lambda_\ell+\sin^2\theta}\right)^{m_\ell} \end{aligned} \tag{33}$$

where m_ℓ is the multiplicity of eigenvalue λ_ℓ. Note that the RHS of (33) has the identical form as the RHS of (28). Therefore, the partial-fraction expansion method, which we discussed in Section IV-A can be directly applied to evaluate the exact-PEP results in closed form.

V. Analytical Performance Evaluation: An Example

As an example, we consider the 4-state QPSK space-time trellis code (STTC) with two transmit antennas proposed by Tarokh *et al.* [1]. The 4-state STTC code is shown in Fig.1 where the labelling of the trellis branches follow [1]. The QPSK signal points are mapped

to the edge label symbols as shown in Fig. 1. For this code, the exact-PEP results and approximate BEP results for $n_R = 1$ and $n_R = 2$ were presented in [4, 6] for i.i.d. fast and slow fading channels. In [7], the effects of spatial fading correlation on the average BEP were studied for $n_R = 1$ over a slow fading channel. In this work, we compare the i.i.d. channel performance results (without considering antenna configurations) presented in [4, 6] with our realistic exact-PEP results for different antenna spacing, antenna placements and scattering distribution parameters.

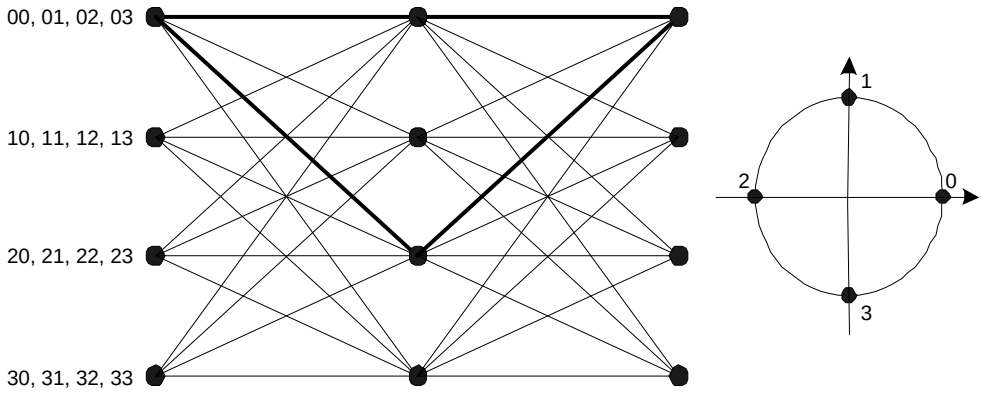

Fig. 1. Trellis diagram for the 4-state space-time code for QPSK constellation.

In [4, 6], performances were obtained under the assumption that the transmitted codeword is the all-zero codeword. Here we also adopt the same assumption as we compare our results with their results. However, we are aware that space-time codes may, in general, be non-linear, i.e., the average BEP can depend on the transmitted codeword.

For the 4-state STTC, we have the shortest error event path of length $H = 2$, as illustrated by shading in Fig. 1 and

$$\boldsymbol{X} = \begin{bmatrix} 1 & 1 \\ 1 & 1 \end{bmatrix}, \quad \hat{\boldsymbol{X}} = \begin{bmatrix} 1 & -1 \\ -1 & 1 \end{bmatrix}. \tag{34}$$

Note that $\boldsymbol{X}$ and $\hat{\boldsymbol{X}}$ in (34) will be used in our simulations.

VI. Effect of Antenna Separation

First we consider the effect of antenna separation on the exact-PEP when the scattering environment is uncorrelated, i.e., $\boldsymbol{F}^T = \boldsymbol{I}_{2M_T+1}$ and $\boldsymbol{F}^R = \boldsymbol{I}_{2M_R+1}$ for the slow fading channel and $\boldsymbol{F}_n^T = \boldsymbol{I}_{2M_T+1}$ and $\boldsymbol{F}_n^R = \boldsymbol{I}_{2M_R+1}$ for the fast fading channel.

A. Slow Fading Channel

Consider the 4-state STTC with $n_T = 2$ transmit antennas and $n_R = 1$ receive antenna. In this case, we place the two transmit antennas in a circular aperture of radius r (antenna separation = $2r$). Since $n_R = 1$, there will only be a single communication mode available at the receiver aperture. Hence $\boldsymbol{J}_R = 1$.

Fig.2 shows the exact pairwise error probability performance of the 4-state STTC for $H = 2$ and transmit antenna separations 0.1λ, 0.2λ, 0.5λ and λ, where λ is the wave-length. Also shown in Fig.2 for comparison is the exact-PEP for the i.i.d. slow fading channel (Rayleigh) corresponding to $H = 2$.

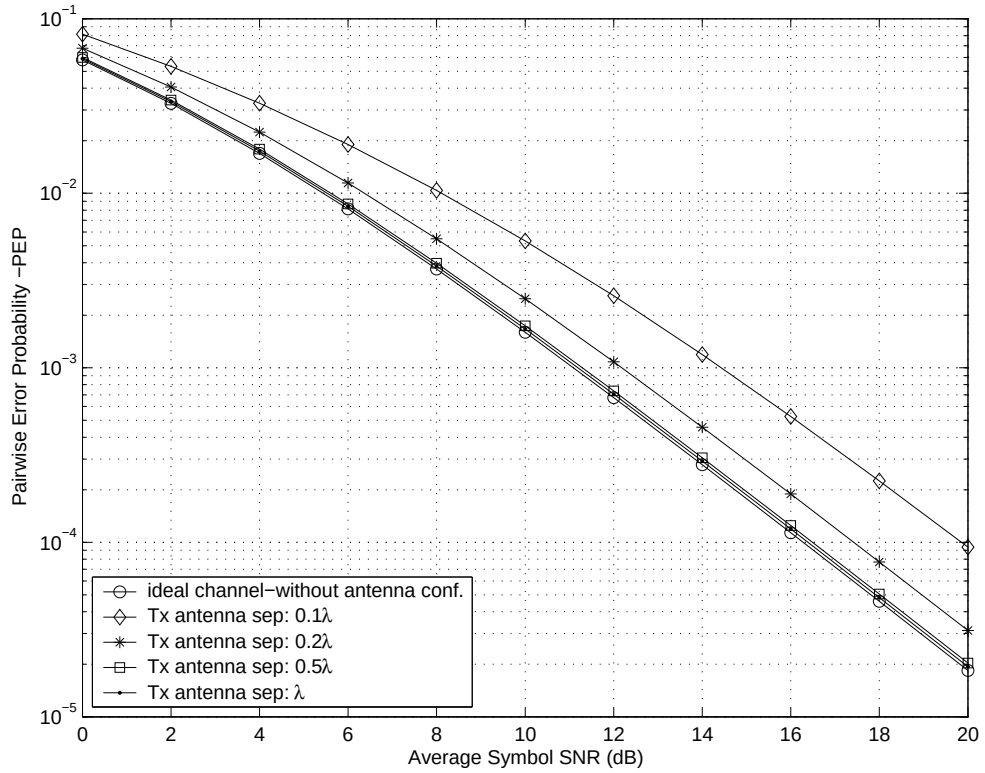

Fig. 2. Exact pairwise error probability performance of the 4-state space-time trellis code with 2-Tx antennas and 1-Rx antenna: length 2 error event, slow fading channel.

As we can see from the figure, the effect of antenna separation on the exact-PEP is not significant when the transmit antenna separation is 0.5λ or higher. However, the effect is significant when the receive antenna separation is small. For example, at 0.2λ and 0.1λ receive antenna separations, the realistic PEPs are 1dB and 3dB away from the i.i.d. channel performance results, respectively. From these observations, we can emphasize that the effect

of antenna spacing on the performance of the 4-state STTC is minimum for higher antenna separations whereas the effect is significant for smaller antenna separations.

1) Loss of Diversity Advantage: We now consider the diversity advantage of a space-time coded system as the number of receive antennas increases while the receive antenna array aperture radius remains fixed. Fig.3 shows the exact-PEP of the 4-state STTC with two transmit antennas and n_R receive antennas, where $n_R = 1, 2, \cdots, 10$. The two transmit antennas are placed in a circular aperture of radius 0.25λ (antenna separation[5] = 0.5λ) and n_R receive antennas are placed in a uniform circular array antenna configuration with radius 0.15λ. In this case, the distance between two adjacent receive antenna elements is $0.3\lambda \sin(\pi/n_R)$.

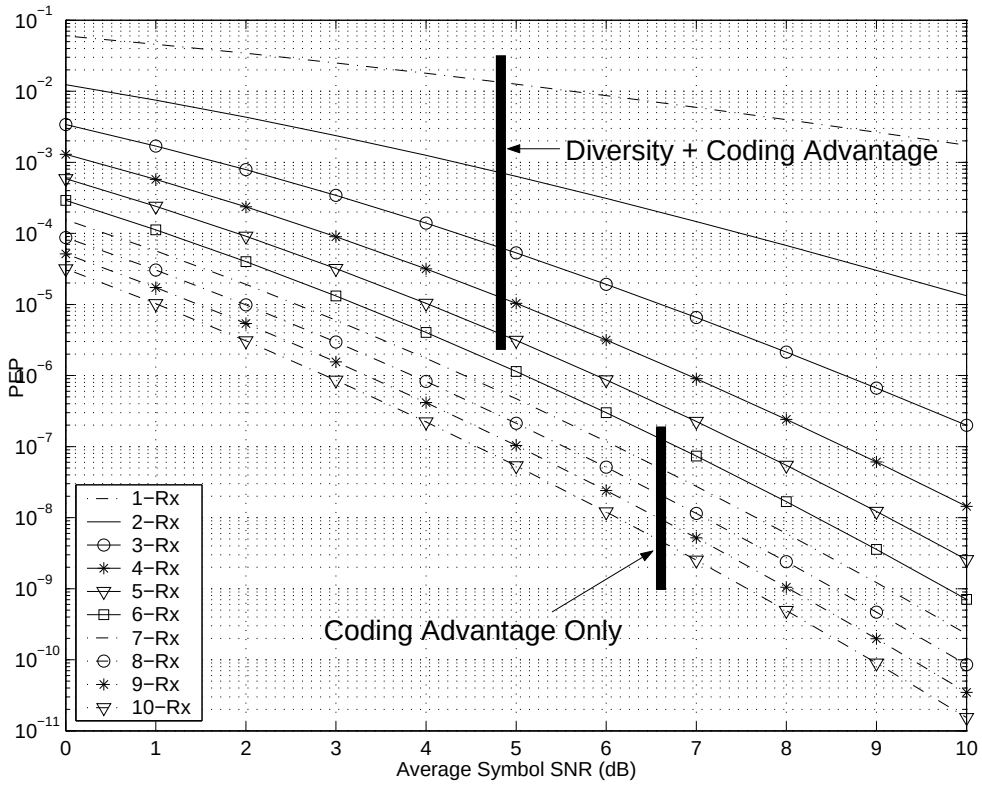

Fig. 3. Exact PEP performance of the 4-state space-time trellis code with 2-Tx antennas and n-Rx antennas: length 2 error event, slow fading channel.

[5]In a 3-dimensional isotropic scattering environment, antenna separation 0.5λ (first null of the order zero spherical Bessel function) gives zero spatial correlation, but here we constraint our analysis to a 2-dimensional scattering environment. The spatial correlation function in a 2-dimensional isotropic scattering environment is given by a Bessel function of the first kind. Therefore, antenna separation $\lambda/2$ does not give zero spatial correlation in a 2-dimensional isotropic scattering environment.

The slope of the performance curve on a log scale corresponds to the diversity advantage of the code and the horizontal shift in the performance curve corresponds to the coding advantage. According to the code construction criteria given in [1], the diversity advantage promised by the 4-state STTC is $2n_R$. With the above antenna configuration setup, however, we observed that the slope of each performance curve remains the same when $n_R > 5$, which results in zero diversity advantage improvement for $n_R > 5$. Nevertheless, for $n_R > 5$, we still observed some improvement in the coding gain, but the rate of improvement is slower with the increase in number of receive antennas. Here the loss of diversity gain is due to the fewer number of effective communication modes available at the receiver region than the number of antennas available for reception. In this case, from (44) in Appendix I, the receive aperture of radius 0.15λ corresponds to $M = 2\lceil \pi e 0.15 \rceil + 1 = 5$ effective communication modes at the receive region. Therefore when $n_R > 5$, the diversity advantage of the code is determined by the number of effective communication modes available at the receiver antenna region rather than the number of antennas available for reception. That is, the point where the diversity loss occurred is clearly related to the size of the antenna aperture, where smaller apertures result in diversity loss of the code for lower number of receive antennas, as proved analytically in [19].

2) Effect of Antenna Configuration: We now compare the exact-PEP results of the 4-state STTC for different antenna configurations at the receiver. For example, we choose UCA and ULA antenna configurations.[6] Consider a system with two transmit antennas and three receive antennas. The two transmit antennas are placed half wavelength ($\lambda/2$) distance apart and the three receive antennas are placed within a fixed circular aperture of radius $r(= 0.15\lambda, 0.25\lambda)$ as shown in Fig.4. The exact-PEP performance for the error event of length two is also plotted in Fig 4.

From Fig.4, it is observed that, the performance given by the UCA antenna configuration outperforms that of the ULA antenna configuration. For example, at 10dB SNR, the performance differences between UCA and ULA are 2.75dB with 0.15λ receiver aperture radius and 1.25dB with 0.25λ receiver aperture radius. Therefore, as we illustrated here, one can use the realistic PEP expressions (24) and (26) to determine the best antenna placement within a given region which gives the maximum performance gain available from a space-time code.

[6]The exact-PEP expressions we derived in this work can be applied to any arbitrary antenna configuration.

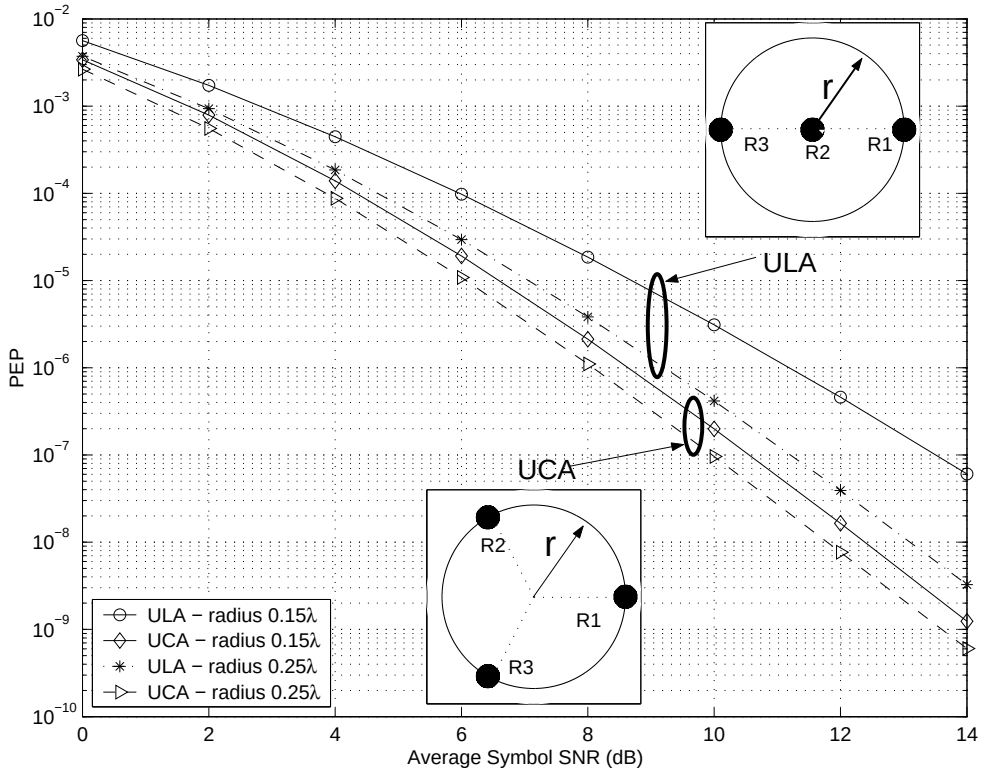

Fig. 4. The exact-PEP performance of the 4-state STTC with two transmit and three receive antennas for UCA and ULA receive antenna configurations: length 2 error event, slow fading channel.

B. Fast Fading Channel

Consider the 4-state STTC with two transmit antennas and two receive antennas, where the two transmit antennas are placed in a circular aperture of radius 0.25λ (antenna separation = 0.5λ) and the two receive antennas are placed in a circular aperture of radius r (antenna separation = $2r$).

Fig.5 shows the exact pairwise error probability performance of the 4-state STTC for $H = 2$ and receive antenna separations 0.1λ, 0.2λ and 0.5λ. Also shown in Fig.5 for comparison, is the exact-PEP for the i.i.d. fast fading channel. Similar results are observed as for the slow fading channel. For the fast fading channel, the effect of antenna separation is minimum when the antenna separation is higher and it is significant when the antenna separation is smaller $(< 0.5\lambda)$. At 0.1λ receive antenna separation, the performance loss is 3dB and at 0.2λ the performance loss is 1dB. Note that the performance loss we observed here is mainly

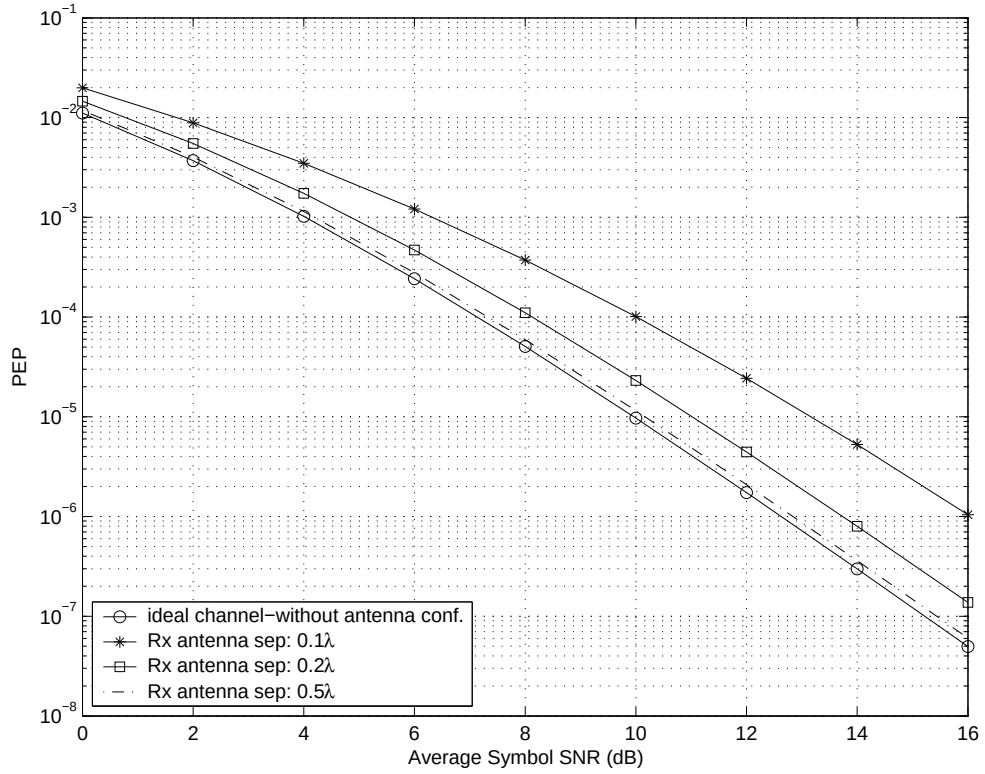

Fig. 5. Exact pairwise error probability performance of the 4-state space-time trellis code with 2-Tx antennas and 2-Rx antennas-length two error event: fast fading channel.

due to the antenna spacing.[7]

VII. Effect of Modal Correlation

In Section VI, we investigated the effect of antenna spacing and antenna configurations on the exact-PEP of space-time codes, assuming an uncorrelated scattering environment. In this section, we study the scattering correlation effects or modal correlation effects on the exact-PEP of space-time codes.

On a fast fading channel environment, we assume that the scattering gains change independently from symbol to symbol. It is also reasonable to assume that the statistics of the scattering channel remain constant over an interval of interest. Here we take the interval of interest as the length of the space-time codeword. Then we have, $\boldsymbol{R}_n = \boldsymbol{R}$ for $n = 1, 2, \cdots, L$ in (14).

[7]Antenna spacing and scattering distribution parameters such as mean AOA/AOD and angular spread are the main contributors to spatial fading correlation.

Using (3), we can define the modal correlation between complex scattering gains as

$$\gamma_{m,m'}^{\ell,\ell'} \triangleq E\left\{\boldsymbol{S}_{\ell,m}\boldsymbol{S}_{\ell',m'}^{*}\right\}.$$

Assume that the scattering from one direction is independent of that from another direction for both the receiver and the transmitter apertures. Then the second-order statistics of the scattering gain function $g(\phi,\varphi)$ can be defined as

$$E\left\{g(\phi,\varphi)g^{*}(\phi^{'},\varphi^{'})\right\} = G(\phi,\varphi)\delta(\phi-\phi^{'})\delta(\varphi-\varphi^{'}),$$

where $G(\phi,\varphi) = E\left\{|g(\phi,\varphi)|^2\right\}$ with normalization $\int\int G(\phi,\varphi)d\varphi d\phi = 1$. With the above assumption, the modal correlation coefficient, $\gamma_{m,m'}^{\ell,\ell'}$ can be simplified to

$$\gamma_{m,m'}^{\ell,\ell'} = \int\int G(\phi,\varphi)e^{-i(\ell-\ell')\varphi}e^{i(m-m')\phi}d\varphi d\phi.$$

Then the correlation between the ℓ-th and ℓ'-th modes at the receiver region due to the m-th mode at the transmitter region is given by

$$\gamma_{\ell,\ell'}^{Rx} = \int \mathcal{P}_{Rx}(\varphi)e^{-i(\ell-\ell')\varphi}d\varphi, \tag{35}$$

where $\mathcal{P}_{Rx}(\varphi) = \int G(\phi,\varphi)d\phi$ is the normalized azimuth power distribution of the scatterers surrounding the receiver antenna region. Here we see that modal correlation at the receiver is independent of the mode selected from the transmitter region.

Similarly, we can write the correlation between the m-th and m'-th modes at the transmitter as

$$\gamma_{m,m'}^{Tx} = \int \mathcal{P}_{Tx}(\phi)e^{i(m-m')\phi}d\phi, \tag{36}$$

where $\mathcal{P}_{Tx}(\phi) = \int G(\phi,\varphi)d\varphi$ is the normalized azimuth power distribution at the transmitter region. As for the receiver modal correlation, we can observe that modal correlation at the transmitter is independent of the mode selected from the receiver region. Note that, azimuth power distributions $\mathcal{P}_{Rx}(\varphi)$ and $\mathcal{P}_{Tx}(\phi)$ can be modeled using all common azimuth power distributions such as Uniform, Gaussian, Laplacian, Von-Mises, etc.

Denoting the p-th column of scattering matrix $\boldsymbol{S}$ as $\boldsymbol{S}_p$, the $(2m_R+1)\times(2m_R+1)$ receiver modal correlation matrix can be defined as

$$\boldsymbol{F}^{R} \triangleq E\left\{\boldsymbol{S}_p\boldsymbol{S}_p^{\dagger}\right\},$$

where the (ℓ, ℓ')-th element of $\boldsymbol{F}^R$ is given by (35) above. Similarly, we can write the transmitter modal correlation matrix as

$$\boldsymbol{F}^T = E\left\{\boldsymbol{S}_q^\dagger \boldsymbol{S}_q\right\},$$

where $\boldsymbol{S}_q$ is the q-th row of $\boldsymbol{S}$. The (m, m')-th element of $\boldsymbol{F}^T$ is given by (36) and $\boldsymbol{F}^T$ is a $(2m_T + 1) \times (2m_T + 1)$ matrix.

The correlation matrix of the scattering channel $\boldsymbol{S}$ can be expressed as the Kronecker product between the receiver modal correlation matrix and the transmitter modal correlation matrix,

$$\boldsymbol{R} = E\left\{\boldsymbol{s}^\dagger \boldsymbol{s}\right\} = \boldsymbol{F}^R \otimes \boldsymbol{F}^T. \tag{37}$$

As a result, the correlation between two distinct modal pairs can be written as the product of corresponding modal correlations at the transmitter and the receiver, i.e.,

$$\gamma_{m,m'}^{\ell,\ell'} = \gamma_{\ell,\ell'}^{Rx} \gamma_{m,m'}^{Tx}. \tag{38}$$

Note that (38) holds only for class of scattering environments where the power spectral density of the modal correlation function satisfies [15, 16]

$$G(\phi, \varphi) = \mathcal{P}_{Tx}(\phi)\mathcal{P}_{Rx}(\varphi). \tag{39}$$

Also note that, (39) is the necessary condition that a channel must satisfy in order to hold the realistic exact-PEP (24) and (26) for the fast and slow fading channels, respectively.

It was shown in [20] that all azimuth power distribution models give very similar correlation values for a given angular spread, especially for small antenna separations. Therefore, without loss of generality, we restrict our investigation only to the Uniform limited azimuth power distribution, which is defined as follows.

***Uniform-limited azimuth power distribution (UL-APD)*:** When the energy is arriving/departing uniformly from/to a restricted range of azimuth angles $\pm\triangle$ around a mean angle of arrival/departure $\omega_0 \in [-\pi, \pi)$, the azimuth power distribution is defined as [21]

$$\mathcal{P}(\omega) = \frac{1}{2\triangle}, \quad |\omega - \omega_0| \leq \triangle, \tag{40}$$

where $\triangle$ represents the non-isotropic parameter of the azimuth power distribution, which is related to the angular spread σ (standard deviation of the distribution). In this case,

$\sigma = \Delta/\sqrt{3}$.

Substituting (40) into (35) gives the receiver modal correlation coefficient

$$\gamma^{Rx}_{\ell,\ell'} = \mathrm{sinc}((\ell - \ell')\Delta_r)e^{-i(\ell-\ell')\varphi_0}, \tag{41}$$

where φ_0 is the mean AOA and Δ_r is the non-isotropic parameter of the azimuth power distribution. Similarly, the modal correlation coefficient at the transmitter is found to be

$$\gamma^{Tx}_{m,m'} = \mathrm{sinc}((m - m')\Delta_t)e^{i(m-m')\phi_0}, \tag{42}$$

where ϕ_0 is the mean AOD and Δ_t is the non-isotropic parameter of the azimuth power distribution.

A. Fast Fading Channel

Consider the 4-state STTC with two transmit antennas and two receive antennas, where the two transmit antennas are separated by a distance of 0.5λ. In Section VI-B, we observed that the performance loss due to antenna separation is minimum when the two receive antenna elements are placed at a distance greater than 0.5λ. Therefore, to study the modal correlation effects on the exact-PEP over a fast fading channel,[8] we set the receive antenna separation to 0.5λ. For simplicity, here we only consider the modal correlation effects at the receiver region and assume that the effective communication modes available at the transmitter region are uncorrelated, i.e., $\boldsymbol{F}^T = \boldsymbol{I}_{2M_T+1}$.

Fig. 6 shows the exact-PEP performances of the 4-state code for various angular spreads $\sigma = \{5^\circ, 30^\circ, 60^\circ, 180^\circ\}$ about a mean AOA $\varphi_0 = 0^\circ$ from broadside, where the broadside angle is defined as the angle perpendicular to the line connecting the two antennas. Note that $\sigma = 180^\circ$ represents the isotropic scattering environment. The exact-PEP performance for the i.i.d. fast fading channel (Rayleigh) is also plotted on the same graph for comparison.

Fig.6 suggests that the performance loss incurred due to the modal correlation increases as the angular spread of the distribution decreases. For example, at 10dB SNR, the realistic PEP performance results obtained from (24) are 0.25dB, 2.5dB, 3.25dB and 7.5dB away from the i.i.d. channel performance results for angular spreads $180^\circ, 60^\circ, 30^\circ$ and 5°, respectively. Therefore, in general, if the angular spread of the distribution is closer to 180° (isotropic

[8]We omit the performance results over a slow fading channel for the sake of brevity.

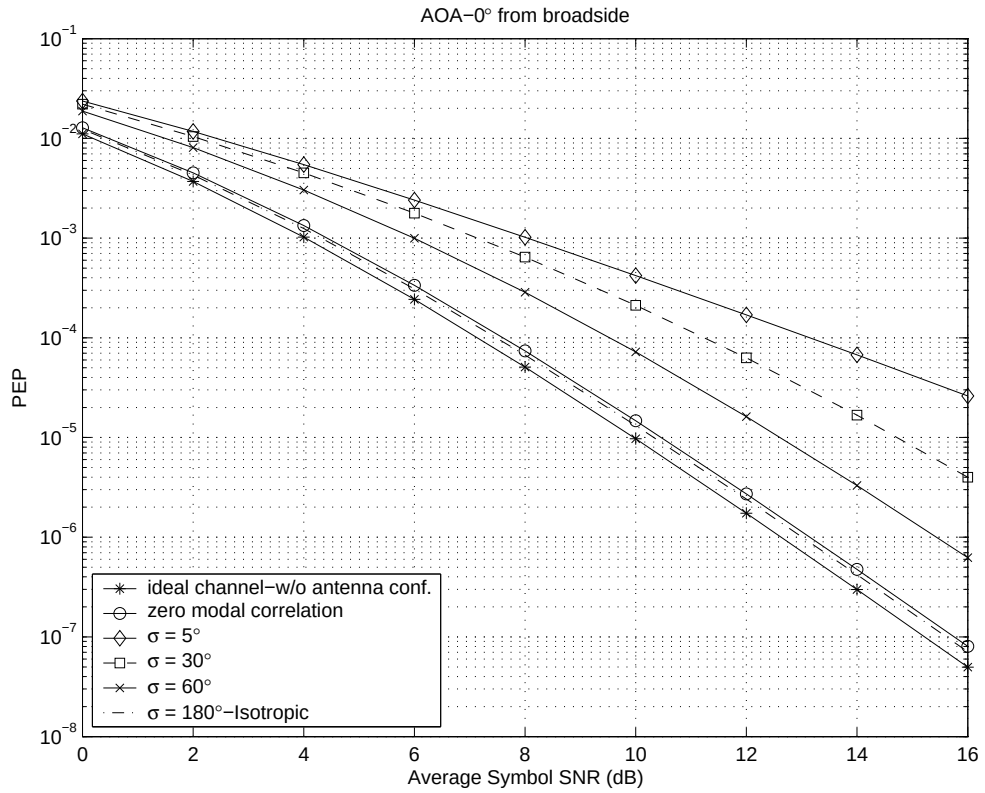

Fig. 6. Effect of receiver modal correlation on the exact-PEP of the 4-state QPSK space-time trellis code with 2-Tx antennas and 2-Rx antennas for the length 2 error event. Uniform limited power distribution with mean angle of arrival 0° from broadside and angular spreads $\sigma = \{5^\circ, 30^\circ, 60^\circ, 180^\circ\}$; fast fading channel.

scattering), then the loss incurred due to the modal correlation is insignificant, provided that the antenna spacing is optimal. However, for moderate angular spread values such as 60° and 30°, the performance loss is quite significant. This is due to the higher concentration of energy closer to the mean AOA for small angular spreads. It is also observed that for large angular spread values, the diversity order of the code (slope of the performance curve) is preserved whereas for small and moderate angular spread values, the diversity order of the code is diminished.

Fig.7 shows the PEP performance results of the 4-state STTC for a mean AOA $\varphi_0 = 45^\circ$ from broadside. Similar results are observed as for the mean AOA $\varphi_0 = 0^\circ$ case. Comparing Figs. 6 and 7 we observe that the performance loss is increased for all angular spreads as the mean AOA moves away from broadside. This can be justified by the reasoning that, as the mean AOA moves away from broadside, there will be a reduction in the angular spread exposed to the antennas and hence less signals being captured.

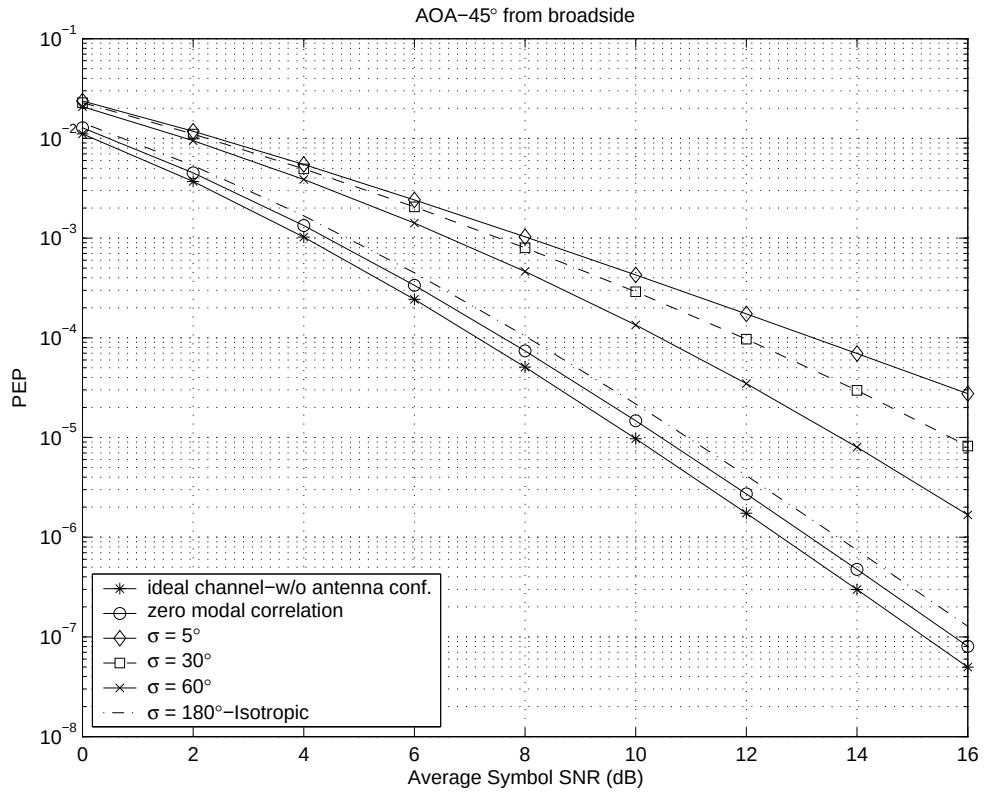

Fig. 7. Effect of receiver modal correlation on the exact-PEP of the 4-state QPSK space-time trellis code with 2-Tx antennas and 2-Rx antennas for the length 2 error event. Uniform limited power distribution with mean angle of arrival 45° from broadside and angular spreads $\sigma = \{5^\circ, 30^\circ, 60^\circ, 180^\circ\}$; fast fading channel.

Finally, we consider the exact-PEP results for the length two error event against the receive antenna separation for a mean AOA $\varphi_0 = 45^\circ$ from broadside and angular spreads $\sigma = [5^\circ, 30^\circ, 180^\circ]$. The results are plotted in Fig.8 for 8dB and 10dB SNRs. It is observed that for a given SNR, the performance of the space-time code is improved as the receive antenna separation and the angular spread are increased. However, the performance does not improve monotonically with the increase in receive antenna separation. We also observed that when the angular spread is quite small (e.g. 5°), we need to place the two receive antenna elements at least several wavelengths apart in order to achieve the maximum performance gain given by the 4-state STTC.

Comparison of Figs. 6, 7 and 8 reveals that when the angular spread of the surrounding azimuth power distribution is closer to 180° (i.e., the scattering environment is near-isotropic), the performance degradation of the code is mainly due to the insufficient antenna spacing. Therefore, employing multiple antennas on a Mobile-Unit (MU) will result in significant

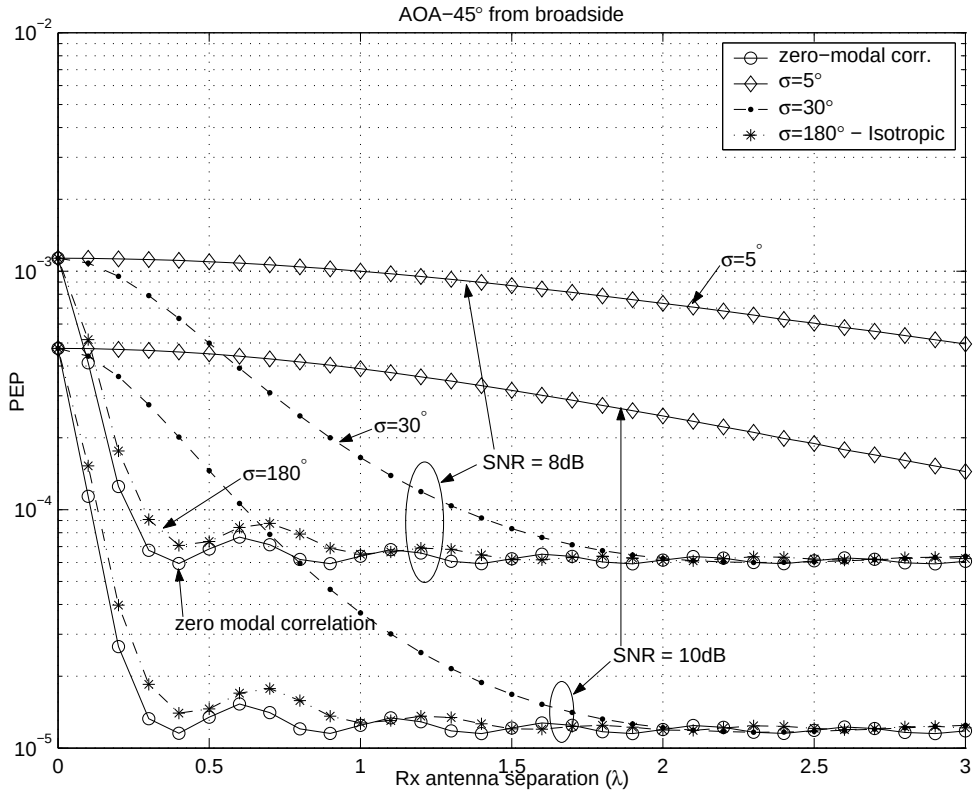

Fig. 8. Exact-PEP of the 4-state QPSK space-time trellis code with 2-Tx antennas and 2-Rx antennas against the receive antenna separation. Uniform limited power distribution with mean angle of arrival 45° from broadside and angular spreads $\sigma = \{5^\circ, 30^\circ, 60^\circ, 180^\circ\}$; fast fading channel

performance loss due to the limited size of the MU.

Furthermore, we observed that (performance results are not shown here) when there are more than two receive antennas in a fixed receive aperture, the performance loss of the 4-state STTC with decreasing angular spread is most pronounced for the ULA antenna configuration when the mean AOA is closer to 90° (inline with the array). But, for the UCA antenna configuration, the performance loss is insignificant as the mean AOA moves away from broadside for all angular spreads. This suggests that the UCA antenna configuration is less sensitive to change of mean AOA compared to the ULA antenna configuration. Hence, the UCA antenna configuration is best suited to employ a space-time code.

Using the results we obtained thus far, we can claim that, in general, space-time trellis codes are susceptible to spatial fading correlation effects, in particular, when the antenna separation and the angular spread are small.

B. Extension of PEP to Average Bit Error Probability

An approximation to the average bit error probability (BEP) was given in [22] on the basis of accounting for error event paths of lengths up to *H* as,

$$\mathrm{P}_b(\boldsymbol{E}) \cong \frac{1}{b}\sum_t q(\boldsymbol{X} \to \hat{\boldsymbol{X}})_t \mathrm{P}(\boldsymbol{X} \to \hat{\boldsymbol{X}})_t, \tag{43}$$

where b is the number of input bits per transmission, $q(\boldsymbol{X} \to \hat{\boldsymbol{X}})_t$ is the number of bit errors associated with the error event t and $\mathrm{P}(\boldsymbol{X} \to \hat{\boldsymbol{X}})_t$ is the corresponding PEP. In [6], it was shown that error event paths of lengths up to *H* are sufficient to achieve a reasonably good approximation to the full upper (union) bound that takes into account error event paths of all lengths. For example, with the 4-state STTC, error event paths of lengths up to $H = 4$ and $H = 3$ are sufficient for the slow and fast fading channels, respectively.

The closed-form solution for average BEP of a space-time code can be obtained by finding closed-form solutions for PEPs associated with each error type, using one of the analytical techniques given in Section IV. In previous sections, we investigate the effects of antenna spacing, antenna geometry and modal correlation on the exact-PEP of a space-time code over fast and slow fading channels. The observations and claims which we made there, are also valid for the BEP case as the BEPs are calculated directly from PEPs. Therefore, to avoid repetition, we do not discuss BEP performance results here.

VIII. CONCLUSION

Using an MGF-based approach, we have derived analytical expressions for the exact-PEP of a space-time coded system over spatially correlated fast and slow fading channels. Two analytical techniques are discussed which can be used to evaluate the exact-PEPs in closed form. The analytical expressions we derived fully account for antenna separation, antenna geometry (Uniform Linear Array, Uniform Grid Array, Uniform Circular Array, etc.) and surrounding azimuth power distributions, both at the receiver and the transmitter antenna array apertures. In practice, these analytical expressions can be used as a tool to estimate or predict the performance of a space-time code under any antenna configuration and surrounding azimuth power distribution parameters. Based on these new PEP expressions, we showed that space-time codes employed on multiple transmit and multiple receive antennas are susceptible to spatial fading correlation effects, particularly for small antenna separations and small angular spreads.

APPENDIX I
TRANSMIT AND RECEIVE ANTENNA ARRAY CONFIGURATION MATRICES

Let $\boldsymbol{u}_p$, $p = 1, 2, \cdots, n_T$ be the position of p-th transmit antenna relative to the transmit antenna array origin and $\boldsymbol{v}_q$, $q = 1, 2, \cdots, n_R$ be the position of q-th receive antenna relative to the receive antenna array origin. Then

$$\boldsymbol{J}_T = \begin{pmatrix} \mathcal{J}_{-m_T}(\boldsymbol{u}_1) & \dots & \mathcal{J}_{m_T}(\boldsymbol{u}_1) \\ \mathcal{J}_{-m_T}(\boldsymbol{u}_2) & \dots & \mathcal{J}_{m_T}(\boldsymbol{u}_2) \\ \vdots & \ddots & \vdots \\ \mathcal{J}_{-m_T}(\boldsymbol{u}_{n_T}) & \dots & \mathcal{J}_{m_T}(\boldsymbol{u}_{n_T}) \end{pmatrix},$$

is the transmit antenna array configuration matrix and

$$\boldsymbol{J}_R = \begin{pmatrix} \mathcal{J}_{-m_R}(\boldsymbol{v}_1) & \dots & \mathcal{J}_{m_R}(\boldsymbol{v}_1) \\ \mathcal{J}_{-m_R}(\boldsymbol{v}_2) & \dots & \mathcal{J}_{m_R}(\boldsymbol{v}_2) \\ \vdots & \ddots & \vdots \\ \mathcal{J}_{-m_R}(\boldsymbol{v}_{n_R}) & \dots & \mathcal{J}_{m_R}(\boldsymbol{v}_{n_R}) \end{pmatrix},$$

is the receive antenna array configuration matrix, where $\mathcal{J}_n(\boldsymbol{x})$ is the spatial-to-mode function (SMF) which maps the antenna location to the n-th mode of the region. The form which the SMF takes is related to the shape of the scatterer-free antenna region. For a circular region in 2-dimensional space, the SMF is given by a Bessel function of the first kind [9] and for a spherical region in 3-dimensional space, the SMF is given by a spherical Bessel function [10]. For a prism-shaped region, the SMF is given by a prolate spheroidal function [23]. Here, we consider only the 2-dimensional scattering environment where antennas are encompassed in scatterer-free circular apertures. Then the SMF is given by

$$\mathcal{J}_n(\boldsymbol{w}) \triangleq J_n(k\|\boldsymbol{w}\|)e^{in(\phi_w - \pi/2)},$$

where $J_n(\cdot)$ is the Bessel function of integer order n, vector $\boldsymbol{w} = (\|\boldsymbol{w}\|, \phi_w)$ in polar coordinates is the antenna location relative to the origin of the aperture which encloses the antennas, $k = 2\pi/\lambda$ is the wave number with λ being the wave length and $i = \sqrt{-1}$.

The number of effective communication modes(M) available in a region is given by [11]

$$M \triangleq 2\lceil \pi e r/\lambda \rceil + 1, \tag{44}$$

where r is the minimum radius of the antenna array aperture and $e \approx 2.7183$.

APPENDIX II
PROOFS

The following three properties of Hermitian matrices will be used to prove that $\boldsymbol{G}_n$ in (10) and $\boldsymbol{G}$ in (20) are Hermitian.

Property 1: If $\boldsymbol{H}$ is any $m \times n$ matrix, then $\boldsymbol{H}\boldsymbol{H}^\dagger$ and $\boldsymbol{H}^\dagger\boldsymbol{H}$ are Hermitian.

Property 2: If $\boldsymbol{A}$ is a Hermitian matrix and $\boldsymbol{H}$ is any matrix, then $\boldsymbol{H}\boldsymbol{A}\boldsymbol{H}^\dagger$ and $\boldsymbol{H}^\dagger\boldsymbol{A}\boldsymbol{H}$ are Hermitian.

Property 3: Kronecker product between two Hermitian matrices are always Hermitian.

Proposition 1: Matrices $\boldsymbol{G}_n = (\boldsymbol{J}_R^\dagger \boldsymbol{J}_R)^T \otimes (\boldsymbol{J}_T^\dagger \boldsymbol{x}_\Delta^n \boldsymbol{J}_T)$ and $\boldsymbol{G} = (\boldsymbol{J}_R^\dagger \boldsymbol{J}_R)^T \otimes (\boldsymbol{J}_T^\dagger \boldsymbol{X}_\Delta \boldsymbol{J}_T)$ are Hermitian, where $\boldsymbol{x}_\Delta^n = (\boldsymbol{x}_n - \hat{\boldsymbol{x}}_n)(\boldsymbol{x}_n - \hat{\boldsymbol{x}}_n)^\dagger$ and $\boldsymbol{X}_\Delta = (\boldsymbol{X} - \hat{\boldsymbol{X}})(\boldsymbol{X} - \hat{\boldsymbol{X}})^\dagger$.

Proof: From *property*-1, matrices $\boldsymbol{J}_R^\dagger \boldsymbol{J}_R$, $\boldsymbol{x}_\Delta^n$ and $\boldsymbol{X}_\Delta$ are Hermitian. Therefore, *property*-2 implies that $\boldsymbol{J}_T^\dagger \boldsymbol{x}_\Delta^n \boldsymbol{J}_T$ and $\boldsymbol{J}_T^\dagger \boldsymbol{X}_\Delta \boldsymbol{J}_T$ are Hermitian. Thus, from *property*-3, $\boldsymbol{G}_n$ and $\boldsymbol{G}$ are Hermitian.

■

REFERENCES

[1] V. Tarokh, N. Seshadri, and A.R. Calderbank, "Space-time codes for high data rate wireless communication: performance criterion and code construction," *IEEE Trans. Info. Theory*, vol. 44, no. 1, pp. 744–765, Mar. 1998.

[2] D.K. Aktas and M.P. Fitz, "Computing the distance spectrum of spacetime trellis codes," in *Proc. Wireless Commun. and Networking Conf. (WCNC'00)*, 2000, vol. 1, pp. 51–55.

[3] R. Gozali and B.D. Woerner, "Upper bounds on the bit-error probability of space-time trellis codes using generating function techniques," in *Proc. IEEE VTC'01 Spring*, Rhodes Island, Greece, 2001, pp. 1318–1323.

[4] M. Uysal and C. N. Georghiades, "Error performance analysis of spacetime codes over rayleigh fading channels," *J. Commun. Networks*, vol. 2, no. 4, pp. 351–355, Dec. 2000.

[5] G.L. Turin, "The characteristic function of hermetian quadratic forms in complex normal random variables," *Biometrika*, vol. 47, no. 1/2, pp. 199–201, June 1960.

[6] M.K. Simon, "Evaluation of average bit error probability for space-time coding based on a simpler exact evaluation of pairwise error probability," *International Journal on Communications and Networks*, vol. 3, no. 3, pp. 257–264, Sept. 2001.

[7] M. Uysal and C. N. Georghiades, "Effect of spatial fading correlation on performance of space-time codes," *Electronics Letters*, vol. 37, no. 3, pp. 181–183, Feb. 2001.

[8] David Gesbert, Helmut Bölcskei, Dhananjay A. Gore, and Arogyaswami J. Paulraj, "Outdoor MIMO wireless channels: Models and performance prediction," *IEEE Trans. Communications*, vol. 50, no. 12, pp. 1926–1934, Dec. 2002.

[9] T.D. Abhayapala, T.S. Pollock, and R.A. Kennedy, "Spatial decomposition of MIMO wireless channels," Paris, France, July 2003, vol. 1, pp. 309–312.

[10] T.D. Abhayapala, T.S. Pollock, and R.A. Kennedy, "Novel 3d spatial wireless channel model," in *IEEE Semiannual Vehicular Technology Conference, VTC2003-Fall*, Oct 2003.

[11] H.M. Jones, R.A. Kennedy, and T.D. Abhayapala, "On dimensionality of multipath fields: Spatial extent and richness," in *Proc. IEEE Int. Conf. Acoust., Speech, Signal Processing, ICASSP'2002*, Orlando, Florida, May 2002, vol. 3, pp. 2837–2840.

[12] J.W. Craig, "A new, simple, and exact result for calculating the probability of error for two-dimensional signal constellations," in *Proc. IEEE MILCOM*, McLean, VA, November 1991, pp. 571–575.

[13] Gene H. Golub and Charles F. Van Loan, *Matrix Computations*, The Johns Hopkins University Press, Baltimore and London, third edition, 1996.

[14] F.D. Neeser and J.L. Massey, "Proper complex random processes with applications to information theory," *IEEE Trans. Info. Theory*, vol. 39, pp. 1293–1302, July 1993.

[15] J.P. Kermoal, L. Schumacher, K.I. Pedersen, P.E. Mogensen, and F. Frederiksen, "A stochastic mimo radio channel model with experimental validation," *IEEE Journal on Selected Areas in Communications*, vol. 20, no. 6, pp. 1211–1226, Aug. 2002.

[16] T.S Pollock, "Correlation Modelling in MIMO Systems: When can we Kronecker?," in *Proc. 5th Australian Communications Theory Workshop*, Newcastle, Australia, February 2004, pp. 149–153.

[17] V.V. Veeravalli, "On performance analysis for signaling on correlated fading channels," *IEEE Trans. Commun.*, vol. 49, no. 11, pp. 1879–1885, Nov. 2001.

[18] M.K. Simon and M.-S. Alouini, *Digital Communications over Fading Channels*, John Wiley & Sons, second edition, to be available November 2004.

[19] T.A. Lamahewa, R.A. Kennedy, and T.D. Abhayapala, "Realistic upper-bound for the pairwise error probability of space-time codes," *Submitted to IEEE Trans. on Wireless Comm.*

[20] T.S. Pollock, T.D. Abhayapala, and R.A. Kennedy, "Introducing space into MIMO capacity calculations," *Journal on Telecommunications Systems*, vol. 24, no. 2, pp. 415–436, 2003.

[21] J. Salz and J.H. Winters, "Effect of fading correlation on adaptive arrays in digital mobile radio," *IEEE Trans. Vehic. Technol.*, vol. 42, no. 4, pp. 1049–1057, Nov. 1994.

[22] J.K. Cavers and P. Ho, "Analysis of the error performance of trellis coded modulations in rayleigh fading channels," *IEEE Trans. Commun.*, vol. 40, no. 1, pp. 74–83, Jan. 1992.

[23] L. Hanlen and M. Fu, "Wireless communications systems with spatial diversity: a volumetric approach," in *IEEE International Conference on Communications, ICC-2003*, 2003, vol. 4, pp. 2673–2677.